

Rosales-Iriarte, F, Fellows, N and Durodola, J (2012) Failure prediction in carbon composites subjected to bearing versus bypass loading.

Rosales-Iriarte, F, Fellows, N and Durodola, J (2012) Failure prediction in carbon composites subjected to bearing versus bypass loading. *Journal of composite materials*, 46 (15). pp. 1859-1878.

Doi: 10.1177/0021998311427766

This version is available: <https://radar.brookes.ac.uk/radar/items/0af51951-2aa2-ad33-b44c-134777603adc/1/>

Available on RADAR: July 2013

Copyright © and Moral Rights are retained by the author(s) and/ or other copyright owners. A copy can be downloaded for personal non-commercial research or study, without prior permission or charge. This item cannot be reproduced or quoted extensively from without first obtaining permission in writing from the copyright holder(s). The content must not be changed in any way or sold commercially in any format or medium without the formal permission of the copyright holders.

This document is the postprint version of the journal article. Some differences between the published version and this version may remain and you are advised to consult the published version if you wish to cite from it.

Failure Prediction in Carbon Composites subjected to Bearing versus Bypass Loading

F. Rosales-Iriarte, N. A. Fellows¹, J. F. Durodola

SMART group, School of Technology, Oxford Brookes University, Wheatley Campus, Wheatley, Oxford, OX33
1HX, UK.

ABSTRACT: To lighten structures many metallic components, such as aircraft wings, are being replaced by composite components. To join these components with the rest of the structure various joining techniques are used. When using multiple bolted joints bypass versus bearing loading is developed around each joint. The ratio of bearing to bypass loading is known to affect the level of load at which failure occurs. There have been many models created to predict failure within composites but very little work has been carried out to investigate how well numerical models predict failure within bolted joints subjected to bearing and bypass loading. In addition few models have been developed that account for the through thickness stresses that are developed underneath the bearing load. This paper compares a range of failure criteria and degradation models utilising a 3 dimensional model and compares how well they predict failure for bearing versus bypass loading for a supported-pin-loaded joint.

KEY WORDS: composite, carbon fibre, damage mechanics, strength prediction, numerical modelling

INTRODUCTION

Multi-fasteners are of interest as they are often used to join composite to metallic structures such as carbon composite aircraft wings onto aluminium fuselages. Multi fastened joints remove the load gradually, with each row of fasteners removing some of the load (bearing load) whilst the remaining load is taken up by the following fasteners (bypass load) [1-4]. This means at each row of joints different ratios of bypass and bearing load exist. A range of diverse numerical and experimental studies have been carried out on these types of joints [5-11]. The main focus of multi-bolted joints has been on predicting the failure strength and determining the best bolt arrangement [8-11]. The numerical work has tended to treat the composite as a 2D laminate thus neglecting the 3D stress state that exists around the pin/bolt hole due to pin/bolt deformation. More recent work has started to

¹ Corresponding author. Tel.: +44 (0) 1865 483503
Email address: nafellows@brookes.ac.uk

model composite bolted joints in 3 dimensions [12-18]. McCarthy et al. [18] for instance looked at bolthole clearance in multi-bolted joints. The work compared results from tests on double lap joints where the bolthole clearances were varied. The predictions of strength were underestimated in the models which the authors put down to the failure criteria and property reduction percentages used in the damage progression analysis. There still appears to be no work carried out on evaluating the effect of varying the bearing versus bypass loading ratio within three dimensional numerical models versus experimental data. One of the reasons for this is that the techniques for testing different ratios of bearing versus bypass are more difficult to perform or require specialised equipment [19, 3]. More recent work by Zarco-González et al. [20, 21], has tried to rectify this by modelling the effect of bearing versus bypass loading on a single pinned composite laminate allowing for the deformation of the pin. Even though the numerical results obtained correlate well with experiments at bearing dominant loads, there is a significant difference in the results at high bypass loads. One of the reasons given by Zarco-González [21] for this is the absence of friction in his modelling work, as well as the failure criteria not being robust enough to cope with the combined effects of tensile and compressive stresses around the hole. From the work carried out for this paper it is believed there is a discrepancy in the results presented by Zarco-González [21] in that the good experimental correlation found at bearing dominant loads are not as good in reality as presented in his work.

A comparison of different failure criteria was carried out in a world wide failure exercise [22, 23]. In this exercise five models were recommended as the most suitable for a wide range of applications but no model was shown to be robust over a wide range of load applications. Many model developers declined to participate in the exercise, including Prof. Z. Hashin [22], on the basis that the models were not able to predict failure in laminates. The advantage of stress based criteria such as Hashin's criteria [24, 25] is that they require limited material data, differentiate between the damage mechanisms, have been validated against a range of problems and can be relatively easily implemented into numerical codes. In order to maintain numerical stability these criteria are often implemented utilising a material degradation model that does not completely degrade the material or degrades the material slowly based on physical properties such as the energy released. Degradation values are controversial as there is often limited physical validity to them and although good results have been obtained for given problems there is doubt about how robust the models will be when subjected to a different type of loading case. Also as the material in the models is not fully degraded some criterion must be used to define when the laminate has completely failed.

Within this paper, the initial work carried out by Zarco-González et al. [20, 21], is taken further by looking at a wide range of currently used stress-based failure criteria and degradation models to evaluate their prediction of damage and ultimate failure in composite pinned joints subjected to bearing versus bypass loads. Although it is known that bolt stress interaction, bolt clearance, clamping force and washer diameter have an effect on joint performance [26], in this case a simple unclamped neat-fit pinned joint was considered to allow comparison with the initial available test data [21] and to reduce the amount of variables to analyse. Friction between the pin and the composite was implemented and different methods were employed to prevent early failure of the models due to numerical instabilities. It is shown that not only is there wide discrepancy among the different failure criteria tested, but also that changes in the post-initial failure degradation model have a significant effect in the ultimate load prediction. In addition, the importance of considering the non-linear and shear terms, the damage parameter and the effect of considering a two or three-dimensional analysis is discussed.

FINITE ELEMENT MODELLING AND PROCEDURE

In his work, Zarco-González [21], carried out a series of experimental bearing versus bypass tests to establish bearing versus bypass curves for a variety of carbon composite laminates. The numerical models presented in this paper used the same materials properties, specimen geometry, see Figure 1, and loading conditions for one of the laminates used in the Zarco-González tests. The laminate was symmetric about a mid plane, running down the centre thickness of the laminate, and made of 16 layers of CFRP, with a nominal thickness of 5mm.

Unfortunately, due to confidentiality the laminate lay-up and properties cannot be disclosed.

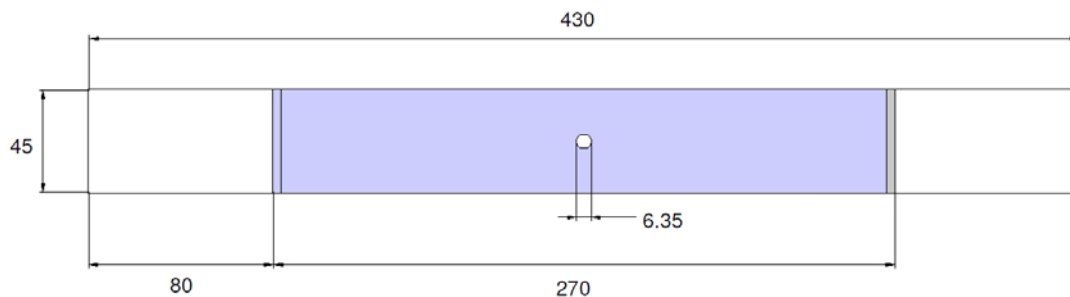


Figure 1 - Specimen dimensions (mm).

Similar to the work of Zarco-González, [21], the USDFLD subroutine within ABAQUS was modified to enable progressive degradation to be applied during a load step. The load applied is divided into increments. Within an increment, iterations are performed in order to find an equilibrium-solution. The code will iterate within the same

increment until finding a solution. At the end of the each increment the structure will be in equilibrium. Within an increment, the failure criteria are evaluated at each integration point of the model. When the stress levels at a given integration point reach critical values as defined by the failure criteria the material properties at that integration point are reduced to reflect that the material at that integration point is damaged. In ABAQUS this is achieved by defining the material properties as a function of field variables. The user subroutine USDFLD within ABAQUS provides the user a method to write a program that updates the field variables at every integration point for each increment in the analysis, according to failure criteria values obtained during the solution. At the beginning of each increment, the user subroutine USDFLD, using the utility subroutine GETVRM, accesses the material point quantities for every integration point in the model. The stress and strains components are then used to compute the failure criterion values. If any of the values are greater or equal to 1 the related field variable for the integration point with the highest failure criterion value is set permanently to 1, indicating failure (It is important to note that degradation models implemented within ABAQUS degrade integration points rather than elements). However the updated values of the field variables do not influence the material properties within the current increment but during the next increment [27]. If more than one integration point field variable is set to fail during an increment the solution becomes explicit, which makes the accuracy of the results dependent on the increment size used. In order to avoid this Zarco-Gonzales [21], selected to fail only the field variable related to the highest failure criterion and used an equilibrium increment between damage increments to re-distribute the stresses. Chang and Chang [28] achieved this by using a Newton-Raphson iteration scheme. However, according to Sleight [29] if a small increment is performed, the step of re-establishing equilibrium may be omitted. This saves computational time and it this approach that has been employed in this work.

Commonly, first order elements are recommended for problems involving contact or large distortions [27], therefore an 8-noded linear brick, reduced integration and hourglass control element (C3D8R) was used in the models within this work. Contact between the pin and the hole and the pin support and laminate surface were modelled using the contact pair approach implemented in ABAQUS with a finite sliding formulation. An important issue related to modelling contact in composite materials is that the coefficient of friction in the contact area might vary depending on the ply orientation. In this instance, Ireman [12] considered the lowest value of friction (0.2 – 0.37) found in tests performed in fractured surfaces in end-notch flexure (ENF) specimens. A similar coefficient of friction (0.2) was considered in the bolt-hole contact zone during all simulations. In

addition, default contact controls were used and the line search algorithm was included to avoid premature increment cut-back due to large residual forces [27]. Symmetric boundary conditions were applied down the centre of the laminate so that only 8 layers of the laminate were modelled (half of the thickness), see Figure 2.

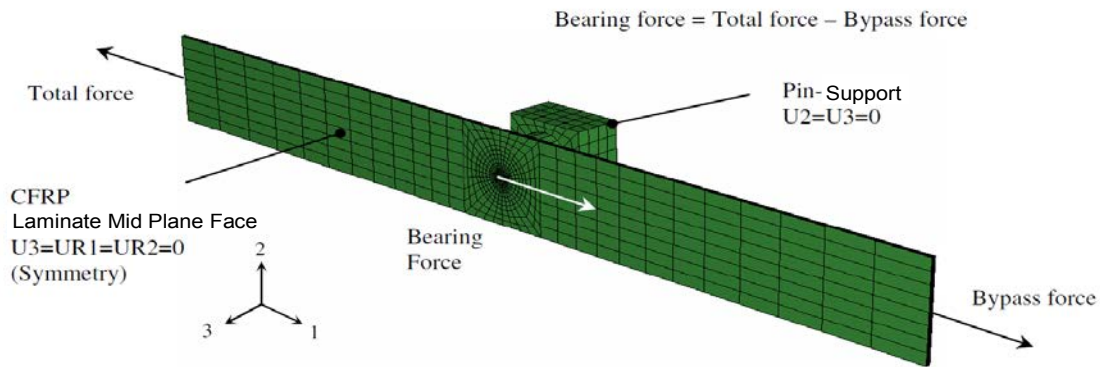


Figure 2 - Laminate and Pin-Support meshing.

Initially the left hand end of the laminate was fixed in the longitudinal direction ($U_1=0$) and a constant pressure was applied to the right hand end (bypass load) whilst the pin and pin support (modelled as one entity) were free to move in the longitudinal direction (low-stiffness springs were applied to the pin to help establish initial contact, see figure 3). A steadily increasing displacement was then applied to the back face of the pin support to induce bearing load in the laminate whilst the pressure (applied in the u_1 direction to the right hand end of the laminate) was kept constant (bypass load). The pin support had a contact diameter of 28mm and was positioned so that it just touched the surface of the composite to replicate the experimental setup. A contact was modelled between the pin support and laminate surface so that it was possible for through thickness stresses to develop during loading due to the laminate expanding laterally under the bearing load.

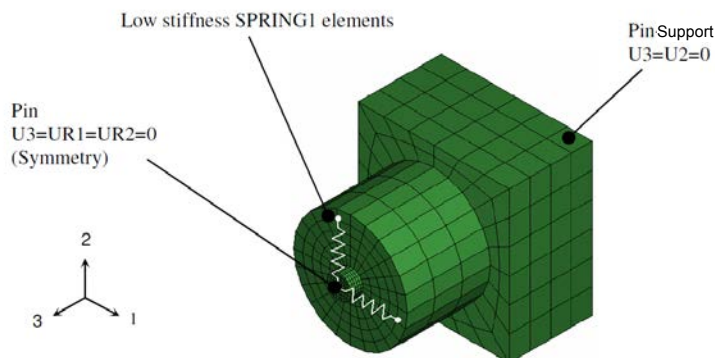


Figure 3 - Pin-Set meshing.

The loads applied to the specimen in the experiments were reproduced in the numerical models. As in the experimental analysis each point of the numerical curve corresponds to an independent bearing versus bypass loading case. Bypass and bearing loads were applied in the same order as in the experimental analysis i.e. a constant bypass load was applied until an equilibrium state was achieved, whereupon bearing load was applied up to laminate failure.

Mesh convergence

The accuracy of the solution from FEA is affected by the mesh size. Too small a mesh will give accurate results at high computational cost but too large a mesh will run quickly but will give inaccurate results. In order to find an optimum mesh size, which gives accurate analytical results for the minimum computational cost, a mesh convergence analysis was carried out. The finite element code used was ABAQUS Standard 6.5. To reduce computational time only half the laminate was modelled. Four models with different element aspect ratios, and mesh densities around the hole were tested, see Figure 4. The longitudinal distance over which the mesh refinement was carried out was equal to the width of the plate. The damage obtained experimentally [21] was within this region. All models were analysed utilising a 20 kN bypass load and a bearing load corresponding to a pin displacement of 0.9368mm. The failure criteria employed for these initial models were those used by Papanikos [30], (Equation 4 and equations 8 to 13).

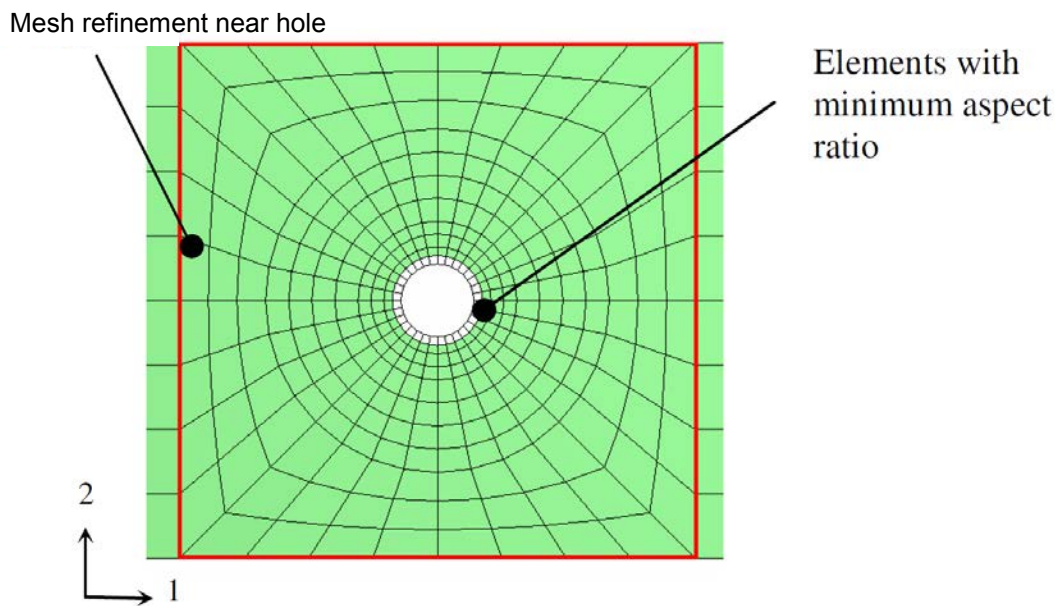


Figure 4 - Finite element model AR3032. Aspect Ratio 3.03.

It was found that the mesh density and aspect ratio affected the final failure load and mesh convergence could not be obtained. It was found that as the mesh density reduced the predicted failure load tended to 25kN. It was decided to use 32 elements around the hole with one element per layer. This gave 256 elements at the hole-boundary and a total of 2816 element in the damage zone. The aspect ratio of the elements around the hole was set to 3.03. Using these settings a failure load of 25.2kN was obtained which gives an error of 0.8% compared to the 25kN trend. A coarser mesh was used away from the hole. The typical mesh, forces and boundary conditions for the laminate and pin-set are shown in Figure 2 and 3.

Failure criteria and degradation models

In composite bolted joints different failure modes can occur depending on the loading conditions and the stress field in the plies. Most of the failure modes can be avoided with careful design, but the net tension and bearing failure modes will still occur depending on the ratio of bearing versus bypass loads. It is important to notice though, that failure modes are affected by joint parameters such as: geometry, laminate lay-up, load direction and bolt clamping forces [31, 32, 33]. Net tension, shear-out and bearing failure modes may occur simultaneously.

When failure is detected in an integration point, the elastic properties in the affected area need to be reduced. The independent elastic properties to be degraded are strongly related to the predicted failure mechanism. This process is controlled through a degradation model. A parametric study performed by Tan [34] showed that the load at which failure occurs in the laminate is very sensitive to the percentage of reduction chosen. Hence, in order to predict the correct damage extension and ultimate failure load not only the ideal failure criteria have to be used, but also a proper degradation model.

As previously mentioned, there have been several failure criteria developed to predict the behaviour of composite laminates under different loading conditions [35, 22, 23]. In this work polynomial stress based criteria have been chosen as they have been shown to give good correlation with a wide range of experimental data and because they are easy to implement in subroutines.

Early theories used a quadratic set of inequalities, which are satisfied when the corresponding combination of stresses are exceeded. Tsai and Wu [36] developed one of the earliest failure criteria. They developed a strength

criterion for anisotropic materials that did not account independently for all the distinct failure modes. Hashin [24, 25] proposed a set of failure criteria for predicting failure of unidirectional composites based on each failure mode. He proposed two failure mechanisms, one based on the failure of the fibre and one based on the failure of the matrix. These failure criteria are expressed in terms of quadratic stress polynomials and according to the author the choice of quadratics is not based on physical reasoning, but on curve fitting considerations [25].

Up to date there have been several researchers that have combined and modified different criteria to form a single set of failure criteria in order to predict damage within a composite laminate. Within this paper, there are 24 equations (Equations 1 to 24) that independently consider the different failure mechanisms, see Table 1. Some of these equations are basically modifications of well-known failure criteria such as Hashin and Rotem [24], Hashin [25], Yamada and Sun [37] and the maximum stress criterion. Modifications include the addition of nonlinear terms and the reduction of shear terms to account for two-dimensional analysis. Ten different sets of failure criteria (combinations of basic criteria and modified criteria) and seven degradation models were used to assess damage in model AR3032. These criteria have been divided into three groups and are discussed in more detail later in the paper.

Table 1 - Failure Criteria Equations.

Matrix Tensile Failure $\sigma_{22} + \sigma_{33} > 0$	$\left(\frac{\sigma_{22} + \sigma_{33}}{Y_t}\right)^2 + \left(\frac{\sigma_{23}^2 - \sigma_{22}\sigma_{33}}{S_T^2}\right) + \left(\frac{\sigma_{12}^2 + \sigma_{13}^2}{S_A^2}\right) \geq 1$	(1)
Matrix Compressive Failure $\sigma_{22} + \sigma_{33} < 0$	$\left[\left(\frac{Y_c}{2S_T}\right)^2 - 1\right]\left(\frac{\sigma_{22} + \sigma_{33}}{Y_c}\right) + \left(\frac{\sigma_{22} + \sigma_{33}}{2S_T}\right)^2 + \left(\frac{\sigma_{23}^2 - \sigma_{22}\sigma_{33}}{S_T^2}\right) + \left(\frac{\sigma_{12}^2 + \sigma_{13}^2}{S_A^2}\right) \geq 1$	(2)
Fibre Tensile Failure $\sigma_{11} > 0$	$\left(\frac{\sigma_{11}}{X_t}\right)^2 + \left(\frac{\sigma_{12}^2 + \sigma_{13}^2}{S_A^2}\right) \geq 1$	(3)
Fibre Compressive Failure $\sigma_{11} < 0$	$\left(\frac{\sigma_{11}}{X_c}\right) \geq 1$	(4)
Matrix Tensile Failure $\sigma_{22} + \sigma_{33} > 0$	$\left(\frac{\sigma_{22} + \sigma_{33}}{Y_t}\right)^2 + \left(\frac{\sigma_{23}^2 - \sigma_{22}\sigma_{33}}{S_T^2}\right) + F_1 \geq 1$ where $F_1 = \frac{2}{G_{12}}(\sigma_{12}^2 + \sigma_{13}^2) + 3\alpha(\sigma_{12}^4 + \sigma_{13}^4)$ $(2S_A^2/G_{12}) + 3\alpha(S_A^4)$	(5)
Matrix Compressive Failure $\sigma_{22} + \sigma_{33} < 0$	$\left[\left(\frac{Y_c}{2S_T}\right)^2 - 1\right]\left(\frac{\sigma_{22} + \sigma_{33}}{Y_c}\right) + \left(\frac{\sigma_{22} + \sigma_{33}}{2S_T}\right)^2 + \left(\frac{\sigma_{23}^2 - \sigma_{22}\sigma_{33}}{S_T^2}\right) + F_1 \geq 1$	(6)
Fibre Tensile Failure $\sigma_{11} > 0$	$\left(\frac{\sigma_{11}}{X_t}\right)^2 + F_1 \geq 1$	(7)
Matrix Tensile Failure $\sigma_{22} > 0$	$\left(\frac{\sigma_{22}}{Y_t}\right)^2 + \left(\frac{\sigma_{12}}{S_{12}}\right)^2 + \left(\frac{\sigma_{23}}{S_{23}}\right)^2 \geq 1$	(8)
Matrix Compressive Failure $\sigma_{22} < 0$	$\left(\frac{\sigma_{22}}{Y_c}\right)^2 + \left(\frac{\sigma_{12}}{S_{12}}\right)^2 + \left(\frac{\sigma_{23}}{S_{23}}\right)^2 \geq 1$	(9)

Fibre Tensile Failure $\sigma_{11} > 0$	$\left(\frac{\sigma_{11}}{X_t}\right) \geq 1$	(10)
Fibre-matrix shear-out Failure $\sigma_{11} < 0$	$\left(\frac{\sigma_{11}}{X_c}\right)^2 + \left(\frac{\sigma_{12}}{S_{12}}\right)^2 + \left(\frac{\sigma_{13}}{S_{13}}\right)^2 \geq 1$	(11)
Delamination in Tension $\sigma_{33} > 0$	$\left(\frac{\sigma_{33}}{Z_t}\right)^2 + \left(\frac{\sigma_{13}}{S_{13}}\right)^2 + \left(\frac{\sigma_{23}}{S_{23}}\right)^2 \geq 1$	(12)
Delamination in Compression $\sigma_{33} < 0$	$\left(\frac{\sigma_{33}}{Z_c}\right)^2 + \left(\frac{\sigma_{13}}{S_{13}}\right)^2 + \left(\frac{\sigma_{23}}{S_{23}}\right)^2 \geq 1$	(13)
Fibre Tensile Failure $\sigma_{11} > 0$	$\left(\frac{\sigma_{11}}{X_t}\right)^2 + \left(\frac{\sigma_{12}}{S_{12}}\right)^2 + \left(\frac{\sigma_{13}}{S_{13}}\right)^2 \geq 1$	(14)
Matrix Tensile Failure $\sigma_{22} > 0$	$\left(\frac{\sigma_{22}}{Y_t}\right)^2 + \left(\frac{\sigma_{12}}{S_T}\right)^2 k_2 = e_m^2$ where $k_2 = \frac{1 + \frac{3}{2}\alpha G_{12}\sigma_{12}^2}{1 + \frac{3}{2}\alpha G_{12}S_c^2}$	(15)
Matrix Compressive Failure $\sigma_{22} < 0$	$\left(\frac{\sigma_{22}}{Y_c}\right)^2 + \left(\frac{\sigma_{12}}{S_T}\right)^2 k_2 = e_m^2$ where $k_2 = \frac{1 + \frac{3}{2}\alpha G_{12}\sigma_{12}^2}{1 + \frac{3}{2}\alpha G_{12}S_c^2}$	(16)
Fibre-matrix shear-out $\sigma_{11} < 0$	$\left(\frac{\sigma_{11}}{X_c}\right)^2 + \left(\frac{\sigma_{12}}{S_T}\right)^2 k_2 = e_{fs}^2$ where $k_2 = \frac{1 + \frac{3}{2}\alpha G_{12}\sigma_{12}^2}{1 + \frac{3}{2}\alpha G_{12}S_c^2}$	(17)
Shear Damage Parameter $\gamma_{12} \neq 0$	$d = \frac{3\alpha G_{12}\sigma_{12}^2 - 2\alpha \frac{G_{12}^3}{\gamma_{12}}}{1 + 3\alpha G_{12}\sigma_{12}^2}$	(18)
Fibre Tensile Failure $\sigma_{11} > 0$	$\left(\frac{\sigma_{11}}{X_t}\right)^2 + \left(\frac{\sigma_{12}}{S_T}\right)^2 k_2 = e_{fs}^2$ where $k_2 = \frac{1 + \frac{3}{2}\alpha G_{12}\sigma_{12}^2}{1 + \frac{3}{2}\alpha G_{12}S_c^2}$	(19)
Fibre Compressive Failure $\sigma_{11} < 0$	$\left(\frac{\sigma_{11}}{X_c}\right)^2 = e_b^2$	(20)
Matrix Tensile Failure $\sigma_{22} > 0$	$\left(\frac{\sigma_{22}}{Y_t}\right)^2 + \left(\frac{\sigma_{12}}{S_T}\right)^2 = e_m^2$	(21)
Matrix Compressive Failure $\sigma_{22} < 0$	$\left(\frac{\sigma_{22}}{Y_c}\right)^2 + \left(\frac{\sigma_{12}}{S_T}\right)^2 = e_m^2$	(22)
Fibre Tensile Failure $\sigma_{11} > 0$	$\left(\frac{\sigma_{11}}{X_t}\right)^2 + \left(\frac{\sigma_{12}}{S_T}\right)^2 = e_{fs}^2$	(23)
Fibre Tensile Failure $\sigma_{11} > 0$	$\left(\frac{\sigma_{11}}{X_t}\right)^2 = e_{fs}^2$	(24)

Where X_t , X_c , Y_t , Y_c , Z_t and Z_c are material strengths (the initial letter represents the direction of the material strength, where X is the fibre direction, Y is the transverse direction and Z is the through thickness direction, and the subscript represents whether it is a tensile or compressive strength), S_A and S_T are the axial and transverse shear stresses, S_{ii} is the shear strength tensor (where ii represents the tensor direction), σ_{ii} is the stress tensor (where ii represents the tensor direction), G_{ii} is the shear modulus tensor (where ii represents the tensor direction), γ_{ii} is the shear damage parameter tensor (where ii represents the tensor direction), α is the shear non linear term and e_m , e_{fs} and e_b are the failure criteria for the matrix tensile or compressive failure, fibre tensile or fibre shear out failure and fibre compressive failure respectively.

Group A

The first group of criteria were taken from McCarthy et al. [18] and O’Higgins et al. [38], see Table 2. The percentage property reduction was set to 90% as proposed by McCarthy et al. [18], which was said by O’Higgins et al., in their work [38], to be based on physical observation.

Table 2 – 3D Hashin Type Failure Criteria.

	3 Dimensional failure criteria			
	Original Hashin	Modified Hashin With shear nonlinear term ^{5, 27, 42}	Hashin fatigue and Ye delamination criteria	Hashin fibre tensile criterion
Criteria	A1	A2	B1	B2
Equations	1-4	4-7	4, 8-13	4, 8-9, 11-14
Degradation Model	1 (Table 3)	1 (Table 3)	2, 3 (Table 4, 5)	2, 3 (Table 4, 5)
Source	[17]	[37]	[29]	[38]

Table 3 - Degradation Model 1 for criteria A1 and A2.

Failure Mechanism	Elastic Properties								
	% Remaining, (*) = 100%								
	E1	E2	E3	v12	v13	v23	G12	G13	G23
NO FAILURE	*	*	*	*	*	*	*	*	*
Matrix tensile / compressive failure	*	10	10	*	*	0	*	*	10
Fibre tensile failure	10	*	*	0	0	*	10	10	*
Fibre compressive failure	10	*	*	0	0	*	10	10	10
Matrix tensile-comp. / Fibre tension	10	10	10	0	0	0	10	10	10
Matrix tensile-comp. / Fibre compressive	10	10	10	0	0	0	10	10	10
All failure	10	10	10	0	0	0	10	10	10

Table 4 - Degradation Model 2 for criteria B1 and B2.

Failure Mechanism	Elastic Properties								
	% Remaining, (*) = 100%								
	E1	E2	E3	v12	v13	v23	G12	G13	G23
NO FAILURE	*	*	*	*	*	*	*	*	*
Matrix tensile failure	*	20	20	*	*	0	*	*	20
Matrix compressive failure	*	40	40	*	*	0	*	*	40
Fibre tensile failure	7	*	*	0	0	*	7	7	*
Fibre compressive failure	14	*	*	0	0	*	14	14	14
Fibre matrix-shear failure	*	*	*	0	0	*	10	10	10
Delamination	*	*	10	*	0	0	*	10	10
Fibre matrix-shear / Delamination	*	*	10	0	0	0	10	10	10
Delamination / Matrix tension failure	*	20	10	*	0	0	*	10	10
Delamination / Matrix tension / Fibre matrix-shear	*	20	10	0	0	0	10	10	10
Fibre matrix-shear / Matrix tension	*	20	20	0	0	0	10	10	10
Delamination / Matrix compression	*	40	10	*	0	0	*	10	10
Delamination / Matrix comp. / Fibre matrix-shear	*	40	10	0	0	0	10	10	10
Fibre matrix-shear / Matrix compression	*	40	40	0	0	0	10	10	10
Fibre matrix-shear / Fibre compression	14	*	*	0	0	*	10	10	10
Delamination / Fibre comp. / Fibre matrix-shear	14	*	10	0	0	0	10	10	10

Delamination / Fibre compression	14	*	10	0	0	0	14	10	10
Matrix tension / Fibre tension	14	20	20	0	0	0	7	7	20
Fib. comp. / Mat. Tension / Delam. / Fibre mat-shear	14	20	10	0	0	0	10	10	10
Matrix tension / Fibre comp. / Fibre matrix-shear	14	20	20	0	0	0	10	10	10
Fibre compression / Matrix tension / Delamination	14	20	10	0	0	0	14	10	10
Matrix tension / Fibre compression	14	20	20	0	0	0	14	14	14
Matrix compression / Fibre comp. / Fibre mat.-shear	14	40	40	0	0	0	10	10	10
Mat. Comp. / Fib. Comp. / Delam. / Fib. Mat.-shear	14	40	10	0	0	0	10	10	10
Matrix compression / Fibre comp. / Delamination	14	40	10	0	0	0	14	10	10
Matrix compression / Fibre compression	14	40	40	0	0	0	14	14	14
Delamination / Fibre tension	7	*	10	0	0	0	7	7	10
Matrix tension / Fibre tension / Delamination	7	20	10	0	0	0	7	7	10
Matrix compression / Fibre tension / Delamination	7	40	10	0	0	0	7	7	10
Matrix compression / Fibre tension	7	40	40	0	0	0	7	7	40

Table 5 - Degradation Model 3 for criteria B1 and B2.

Failure Mechanism	Elastic Properties								
	% Remaining, (*) = 100%								
	E1	E2	E3	v12	v13	v23	G12	G13	G23
NO FAILURE	*	*	*	*	*	*	*	*	*
Matrix tensile failure	*	10	10	0	*	0	10	*	10
Matrix compressive failure	*	10	10	0	*	0	10	*	10
Fibre tensile failure	10	*	*	0	0	*	*	10	*
Fibre compressive failure	10	*	*	0	0	*	*	10	10
Fibre matrix-shear failure	*	*	*	0	0	*	10	10	10
Delamination	*	*	10	*	0	0	*	10	10
Matrix tension / Fibre tension	10	10	10	0	0	0	10	10	10
Matrix tension / Fibre compression	10	10	10	0	0	0	10	10	10
Matrix compression / Fibre tension	10	10	10	0	0	0	10	10	10
Matrix compression / Fibre compression	10	10	10	0	0	0	10	10	10
Delamination / Matrix tension failure	*	10	10	0	0	0	10	10	10
Delamination / Matrix compression	*	10	10	0	0	0	10	10	10
Delamination / Fibre tension	10	*	10	0	0	0	*	10	10
Delamination / Fibre compression	10	*	10	0	0	0	*	10	10
Fibre matrix-shear / Matrix tension	*	10	10	0	0	0	10	10	10
Fibre matrix-shear / Matrix compression	*	10	10	0	0	0	10	10	10
Fibre matrix-shear / Delamination	*	*	10	0	0	0	10	10	10
Fibre matrix-shear / Fibre compression	10	*	*	0	0	*	10	10	10
Matrix tension / Fibre tension / Delamination	10	10	10	0	0	0	10	10	10
Matrix tension / Fibre compression / Fibre matrix-shear	10	10	10	0	0	0	10	10	10
Matrix compression / Fibre tension / Delamination	10	10	10	0	0	0	10	10	10
Matrix compression / Fibre compression / Delamination	10	10	10	0	0	0	10	10	10
Matrix compression / Fibre comp. / Fibre matrix-shear	10	10	10	0	0	0	10	10	10

Fibre compression / Matrix tension / Delamination	10	10	10	0	0	0	10	10	10
Delamination / Matrix tension / Fibre matrix-shear	*	10	10	0	0	0	10	10	10
Delamination / Matrix compression / Fibre matrix-shear	*	10	10	0	0	0	10	10	10
Delamination / Fibre compression / Fibre matrix-shear	10	*	10	0	0	0	10	10	10
Mat. Comp. / Fib. Comp. / Delam. / Fibre matrix-shear	10	10	10	0	0	0	10	10	10
Fib. comp. / Mat. tension / Delam. / Fibre mat-shear	10	10	10	0	0	0	10	10	10

Group B

The criteria in group B are taken from the work of Papanikos et al. [30] and Tserpes et al. [43], see Table 2. Two degradation models were used. Degradation model 2 is based on the work of Papanikos et al. [30] and degradation model 3 was based on the work of McCarthy et al. [18] and Dano et al. [44]. The degradation model proposed by Tserpes et al. [43] was not used.

Group C

The group C criteria are based on two-dimensional Hashin-type failure criteria taken from Dano et. al. [44] and Chang and Lessard [46], see Table 6. Chang and Lessard [46] used a degradation model that reduced the material properties to zero for open holed composites. When this level of degradation was applied to models of pin-loaded composite joints, developed in ABAQUS, premature abortion occurred, Zarco-González [21]. The degradation models therefore used, as proposed by Zarco-González [21] and Dano et al. [44], reduced the material properties by 90%.

Table 6 – 2D Hashin Type Failure Criteria.

	2 Dimensional Hashin type failure criteria			
	Yamada - Sun criterion ³⁶ , Hahn –Tsai ⁵¹	Five failure modes	No fibre matrix shear out failure	No nonlinear shear strain criterion
Criteria	C1	C2	C3	C4
Equations	15-18	15-20	15-16, 18-20	15-16, 18, 20, 24
Degradation Model	4 (Table 7)	5 (Table 8)	6 (Table 9)	6 (Table 9)
Source	[40]	[39]	[39]	[39]

In order to assess the independent effect of the shear non-linear behaviour and the non-linear damage parameter (damage accumulation), criteria C3 was modified in this work, see Table 10. Criteria C3A do not take into account any non-linear effect whereas criteria C3B and C3C considered the non-linear shear behaviour and the non-linear shear stress-strain relationship respectively. Criteria C4 are very similar to criteria C3, but the fibre tensile failure criterion (equation 24) does not include the shear term (equation 19).

Table 7 - Degradation Model 4 for criteria C1.

Failure Mechanism	Elastic Properties								
	% Remaining, (*) = 100%								
	E1	E2	E3	v12	v13	v23	G12	G13	G23
NO FAILURE	*	*	*	*	*	*	*	*	*
Matrix tensile / compressive failure	*	10	10	0	0	*	*	*	*
Fibre matrix shear	*	*	*	0	0	*	10	10	10
Damage	*	*	*	*	*	*	10	10	10
Matrix tensile-comp./ Fibre mat.-shear	*	10	10	0	0	*	10	10	10
Matrix tensile-comp./ Damage	*	10	10	0	0	*	10	10	10
Fibre mat.-shear / damage	*	*	*	0	0	*	10	10	10
All failure	*	10	10	0	0	*	10	10	10

Table 8 - Degradation Model 5 for criteria C2.

Failure Mechanism	Elastic Properties								
	% Remaining, (*) = 100%								
	E1	E2	E3	v12	v13	v23	G12	G13	G23
NO FAILURE	*	*	*	*	*	*	*	*	*
Matrix tensile failure	*	10	10	10	*	10	10	*	10
Matrix compressive failure	*	10	10	10	*	10	10	*	10
Fibre matrix-shear failure	*	*	*	10	10	*	10	10	10
Fibre tensile failure	10	*	*	10	10	*	*	10	*
Fibre compressive failure	10	*	*	10	10	*	*	10	10
Damage	*	*	*	*	*	*	10	10	10
Matrix tension / Fibre tension	10	10	10	10	10	10	10	10	10
Matrix tension / Fibre compression	10	10	10	10	10	10	10	10	10
Matrix compression / Fibre tension	10	10	10	10	10	10	10	10	10
Matrix compression / Fibre compression	10	10	10	10	10	10	10	10	10
Damage / Matrix tension failure	*	10	10	10	*	10	10	10	10
Damage / Matrix compression	*	10	10	10	*	10	10	10	10
Damage / Fibre tension	10	*	*	10	10	*	10	10	10
Damage / Fibre compression	10	*	*	10	10	*	10	10	10
Fibre matrix-shear / Matrix tension	*	10	10	10	10	10	10	10	10
Fibre matrix-shear / Matrix compression	*	10	10	10	10	10	10	10	10
Fibre matrix-shear / Damage	*	*	*	10	10	*	10	10	10
Fibre matrix-shear / Fibre compression	10	*	*	10	10	*	10	10	10
Matrix tension / Fibre tension / Damage	10	10	10	10	10	10	10	10	10
Matrix tension / Fibre comp. / Fibre matrix-shear	10	10	10	10	10	10	10	10	10
Matrix compression / Fibre tension / Damage	10	10	10	10	10	10	10	10	10
Matrix compression / Fibre compression / Damage	10	10	10	10	10	10	10	10	10
Matrix comp. / Fibre compression / Fibre matrix-shear	10	10	10	10	10	10	10	10	10
Fibre compression / Matrix tension / Damage	10	10	10	10	10	10	10	10	10
Damage / Matrix tension / Fibre matrix-shear	*	10	10	10	10	10	10	10	10
Damage / Matrix compression / Fibre matrix-shear	*	10	10	10	10	10	10	10	10
Damage / Fibre compression / Fibre matrix-shear	10	*	*	10	10	*	10	10	10

Mat. Comp. / Fib. Comp. / Damage / Fibre mat.-shear	10	10	10	10	10	10	10	10	10
Fib. comp. / Mat. tension / Damage / Fibre mat.-shear	10	10	10	10	10	10	10	10	10

Table 9 - Degradation Model 6 for criteria C3, C4 and C3C.

Failure Mechanism	Elastic Properties								
	% Remaining, (*) = 100%								
	E1	E2	E3	v12	v13	v23	G12	G13	G23
NO FAILURE	*	*	*	*	*	*	*	*	*
Matrix tensile failure	*	10	10	10	*	10	10	*	10
Matrix compressive failure	*	10	10	10	*	10	10	*	10
Fibre tensile failure	10	*	*	10	10	*	*	10	*
Fibre compressive failure	10	*	*	10	10	*	*	10	10
Damage	*	*	*	*	*	*	10	10	10
Matrix tension / Fibre tension	10	10	10	10	10	10	10	10	10
Matrix tension / Fibre compression	10	10	10	10	10	10	10	10	10
Matrix compression / Fibre tension	10	10	10	10	10	10	10	10	10
Matrix compression / Fibre compression	10	10	10	10	10	10	10	10	10
Damage / Matrix tension failure	*	10	10	10	*	10	10	10	10
Damage / Matrix compression	*	10	10	10	*	10	10	10	10
Damage / Fibre tension	10	*	*	10	10	*	10	10	10
Damage / Fibre compression	10	*	*	10	10	*	10	10	10
Matrix tension / Fibre tension / Damage	10	10	10	10	10	10	10	10	10
Matrix comp. / Fibre tension / Damage	10	10	10	10	10	10	10	10	10
Matrix comp. / Fibre comp. / Damage	10	10	10	10	10	10	10	10	10
Fibre comp. / Matrix tension / Damage	10	10	10	10	10	10	10	10	10

Table 10 – Modified 2D Hashin Type Failure Criteria to see effect of non-linear terms.

	2 Dimensional Hashin type failure criteria		
	No Nonlinearity	Shear Stress Nonlinearity	Shear Strain Nonlinearity
Criteria	C3A	C3B	C3C
Equations	20-23	15-16, 19-20	18,20-23
Degradation Model	7 (Table 10)	7 (Table 10)	6 (Table 9)
Source	New	New	New

Table 11 - Degradation model 7 for criteria C3A and C3B.

Failure Mechanism	Elastic Properties								
	% Remaining, (*) = 100%								
	E1	E2	E3	v12	v13	v23	G12	G13	G23
NO FAILURE	*	*	*	*	*	*	*	*	*
Matrix tensile failure	*	10	10	0	*	0	10	*	10
Matrix compressive failure	*	10	10	0	*	0	10	*	10
Fibre tensile failure	10	*	*	0	0	*	*	10	*

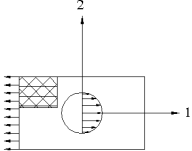
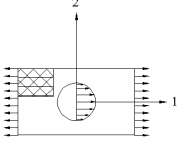
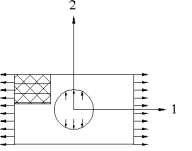

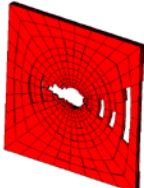
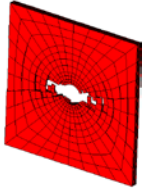
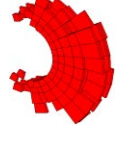
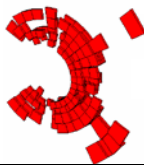
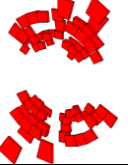



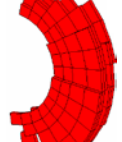
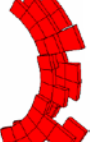
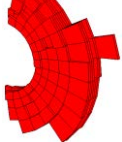
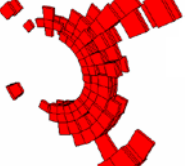
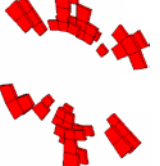
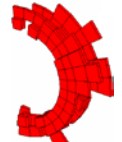
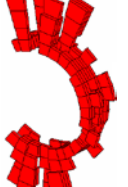
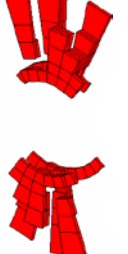
Fibre compressive failure	10	*	*	0	0	*	*	10	10
Matrix tension / Fibre tension	10	10	10	0	0	0	10	10	10
Matrix tension / Fibre compression	10	10	10	0	0	0	10	10	10
Matrix compression / Fibre tension	10	10	10	0	0	0	10	10	10
Matrix compression / Fibre compression	10	10	10	0	0	0	10	10	10

NUMERICAL ANALYSIS

The numerical model and procedure, discussed in the previous section, were used to perform a comparison among the different failure criteria. In Table 12 the damage generated due to different loading cases is presented. The models were stopped when damage in the load bearing layers (fibres aligned longitudinally) reached 3.5mm (approximately 4 elements). In pure bearing the models stopped due to the fibre compressive failure damage reaching this criterion and in the 50kN bypass and the pure bypass case the models stopped due to the fibre tensile failure damage reaching this criterion. The reasons the 3.5mm criterion was used are discussed in more detail below.

Several researchers have considered fibre tensile or compressive failure as the most important failure mechanism when considering final failure [22, 23]. This is because most of the time the stiffness of the fibre is much higher than that of the matrix. In Table 12, high amounts of fibre and matrix damaged elements are observed. Since fibres are the main load carrying elements, the laminate is considered damaged when fibres undergo a certain extent of damage, as explained later. For the combined bearing-bypass load case the fibre tensile failure mechanism is dominant. It is found that as the bearing force becomes dominant the fibre tensile failure mode diminishes and as bypass force becomes dominant the fibre compressive failure damage diminishes, which is to be expected. Another important failure mechanism present is de-lamination. This failure mechanism was induced by the compressive forces acting in the pin-hole contact, where the out-of-plane stresses increased and forced the fibres to split out.

Table 12 - Damage extension around the hole due to different failure mechanisms for three bearing-bypass loading cases. Criteria B1 degradation model 2.

	Pure Bearing Load	13.364 kN Bearing Load 50 kN Bypass Load	Pure Bypass Load
Loading case			
Matrix tensile failure			
Matrix compressive failure			
Fibre tensile failure			
Fibre compressive failure			No damage
Fibre matrix-shear			
Delamination			

It is important to point out that assessing ultimate failure within a composite numerical analysis is difficult and must be judged with great care. It has been observed in work performed by Tserpes et al [47], and Dano et al [44], that researchers have taken different approaches when selecting the failure load point. The Characteristic Curve Method [39] and the Failure Area Index method [48] use the stress field with some failure criteria to determine failure. The CCM sets failure as being the point at which the selected failure criterion is exceeded at any point on the characteristic curve on any ply. The FAI method sums up failure values on each ply, and then across the plies, to obtain an overall FAI value. This value is compared to an FAI obtained from a stress field generated numerically, using an experimentally obtained failure load, to determine failure. For progressive models the approaches include: a characteristic failure distance for bearing load defined by geometric parameters of the joint [49], or defined by the outer diameter of the washer in a bolted joint [50, 43], the first peak in a load displacement curve [51, 52, 12], the half of the maximum load just prior to unstable non-linear behaviour [53] among others. The reason that this is sometime required with some progressive damage models is that in order to get numerical stability the material properties are given residual material properties after failure which can mask physical instabilities.

The model as proposed by Hung and Chang [49] is very appealing as it implements a damage parameter that reduces the laminate stiffness dramatically when the damage area reaches a critical value. The criterion uses two experimental parameters that were found to be reasonably insensitive to load conditions but were developed for bearing load (with and without bolt pre-load). Ascione et al. [54, 55] have developed a semi-empirical formula for predicting the failure load with varying lamina directions and bolt diameter based on carrying out three experimental tests with different lamina orientations. In this work both bearing and bypass loads were applied with the additional complication that the laminate was semi-clamped with the pressure varying under the pin support as the load was increased. It was therefore decided, knowing that the distance from the hole at which damage causes final failure is geometry and material dependant, to determine the distance from the hole at which damage increased rapidly. This rapid damage growth, sometimes indicated by a flat slope or a drop in load, was evident in most cases but was easier to pick out for some failure criteria than others and was not evident for pure bearing loads. It was found that this rapid growth in damage occurred when the fibre tensile damage or compressive damage extended 3.5mm in any direction from the hole. Similar observations were made by O'Higgins et al. [38], however they did not consider a damaged extension distance as the final failure point. The

reason why damage developed in some cases without any clear signal of laminate rupture might be due to the fact that although the stiffness of failed elements is reduced when they fail, it is not reduced to zero. This is to prevent the models becoming unstable but this means that the elements can still support load which will cause the overall load supported by the laminate to keep increasing as the loading continues even though the damage has become extensive. In reality, although there may be some residual strength in failed material due to friction and interweaving of failed strands, the strength is going to be very low after failure and significantly lower than used in the degradation models. To see the effect of reducing the material strength to zero, models were run where failed elements were manually deleted before applying increased load. Although element deletion is supported in ABAQUS standard it is not a straight forward task to use it with a damage progression analysis. In order to perform an analysis with this feature, the elements to be deleted have to be known prior to the analysis, but this is not possible until an analysis is performed. An initial analysis is therefore required to determine which elements require deleting. A subsequent analysis fails the element with the highest failure criteria value. These two analyses are then repeated until at the set load there are no further elements exceeding the failure criteria. It was observed that at 3.5 mm away from the hole-edge the elements kept failing without applying any extra load. If element deletion is stopped and extra load or displacement is applied the curve will start increasing again, see Figure 5. Figure 5 also shows the difference between elastic property degradation and element deletion. Element deletion is only possible to perform when there is no contact between parts, since failed elements underneath the bolt have to remain in order to account for crushed material.

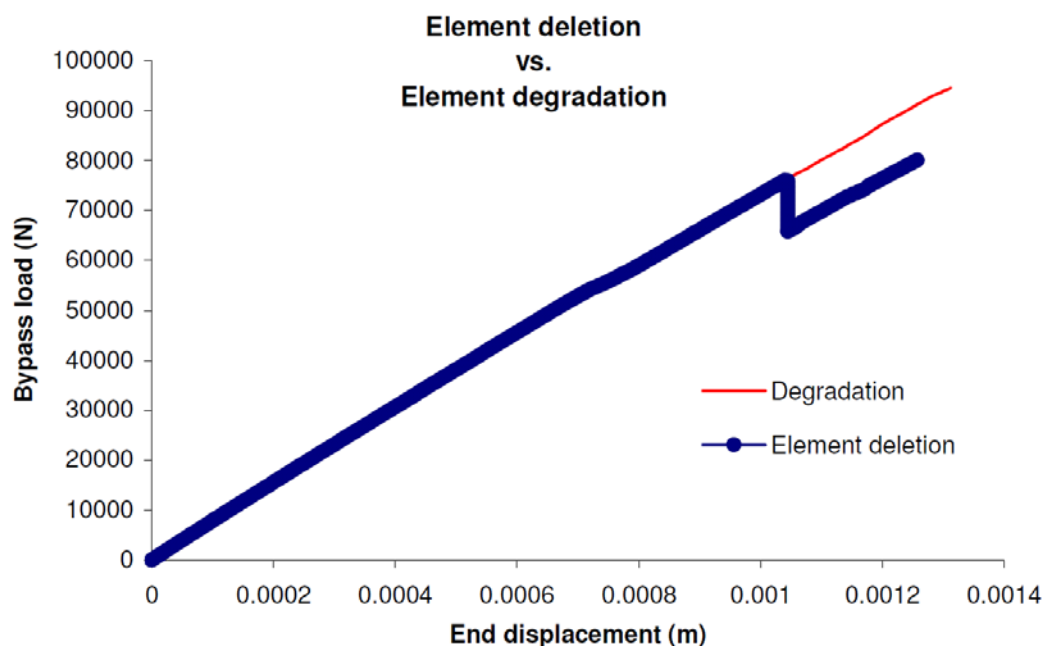


Figure 5 - Comparison between bypass curves with element properties degradation and element deletion.

Based on the damage growth results and element deletion model results the laminates were considered to fail when the damage extension in the main load carrying layers reached a radial distance of 3.5 mm away from the hole-edge. This was done to provide consistency in comparing the different failure criteria and to speed up the analysis process. It is important to mention that this distance will be laminate geometry and hole-diameter dependent. The method utilised though is not empirical, although validated against experimental data, as the distance can be found numerically, by picking the distance at which damage rapidly increases and verifying using an element deletion model. To check that this distance was not determined by the mesh size different mesh densities were utilised with similar results.

Unfortunately, not all the material properties were available for the material analysed in this study, and the transverse and out-of-plane shear strengths were considered similar to the in-plane shear strength, i.e.

$S_{12}=S_{13}=S_{23}$.

RESULTS

Group A

The Hashin's three-dimensional criteria and Hashin's modified criteria, A1 and A2 respectively, produced very similar curves, see Figure 6. Nonetheless, criteria A2, which includes the non-linear shear behaviour term, gave higher (better) failure load predictions than its counterpart A1. Both sets under-predicted failure for bearing and bypass loads.

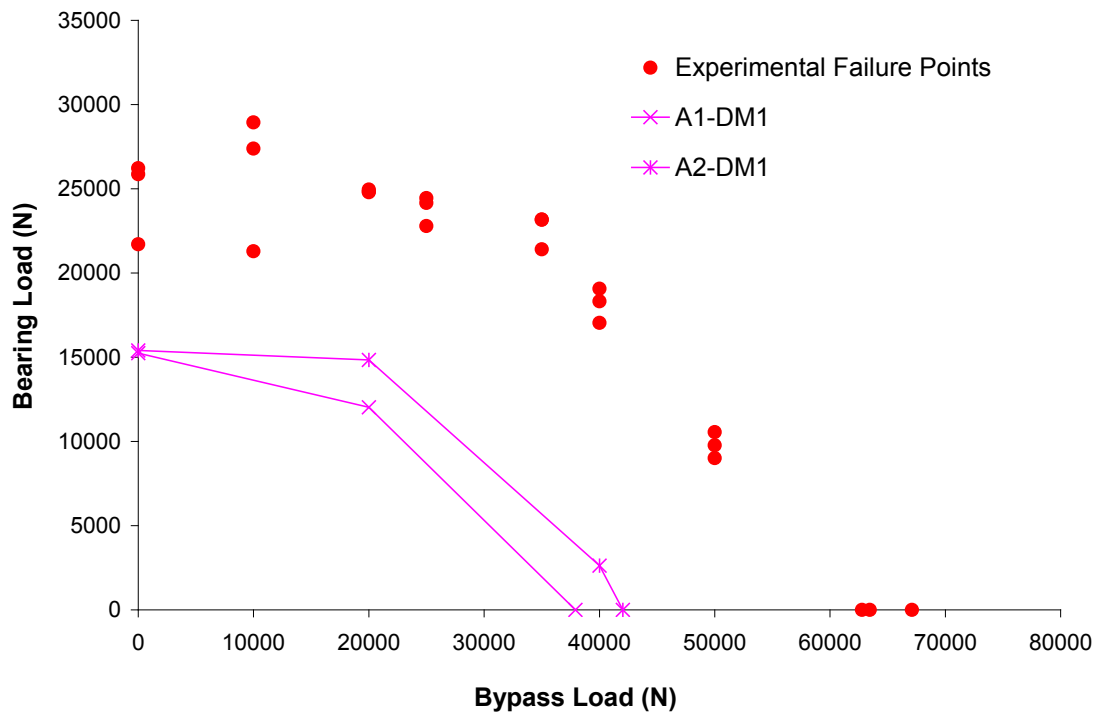


Figure 6 - Bearing versus bypass curves for group A. Original three-dimensional Hashin failure criteria. Degradation model 1.

The effect of the shear non-linearity term is to reduce the effect the shear stress has in the criteria and therefore enables the laminate to support more load. McCarthy et al. [18], also found that ultimate bearing load was under-predicted by criteria A1. They attributed this under-prediction to the degradation model employed and to the fact that the non-linear shear behaviour of the laminate was sensitive to the failure criteria chosen. On the other hand O'Higgins et al. [38], using criteria A2, found that the ultimate failure loads for laminates with open-holes subjected to tensile forces agreed well with experimental results. One of the reasons for this might be due to the fact that the models were two-dimensional and out-of-plane stresses were not considered.

Group B

The only difference between criteria B1 and B2 is the fibre tensile criterion. Criteria B1 use the maximum stress criterion (equation 10) whereas B2 uses the Hashin type failure criterion (equation 14). When using degradation model 2, both criteria sets gave reasonable results for the pure bearing case (compressive stresses are dominant). However, it is clear that as soon as tensile stresses become higher (and therefore the shear stresses), the shear term in the fibre tensile criterion of criteria B2 causes the element to fail prematurely, see Figure 7. This observation agrees with that made by Tserpes et al. [47]. The lack of the shear term in the fibre tensile criterion of B1 (equation 10) allows the laminate to support more tensile load.

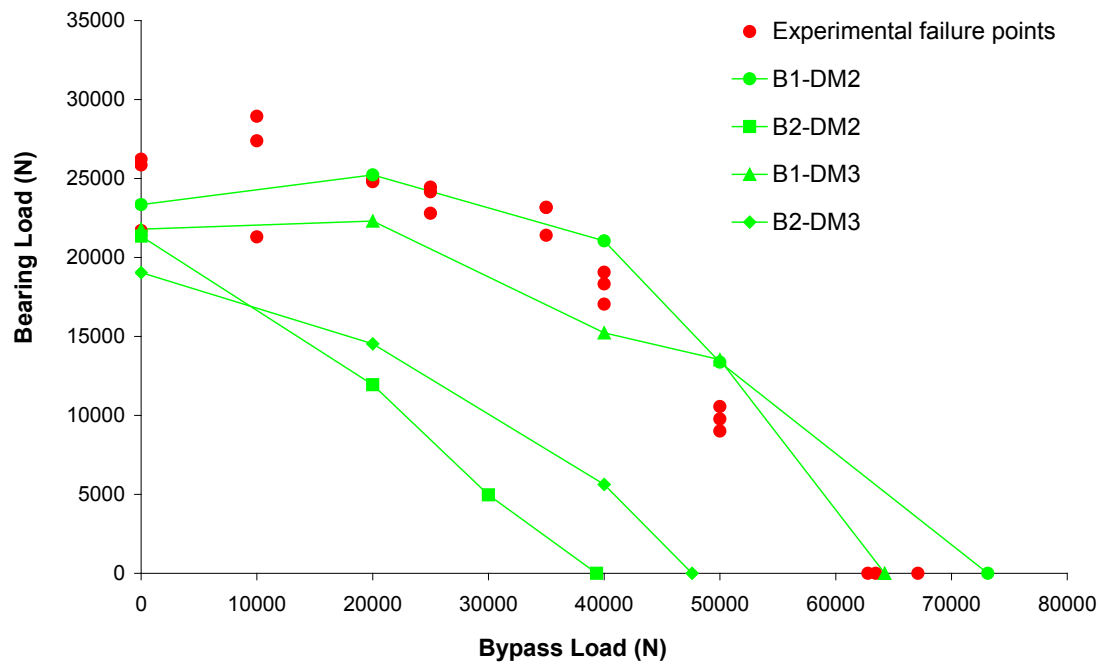


Figure 7 - Bearing versus bypass curves for group B. Three-dimensional Hashin type failure criteria. Degradation models 2 and 3.

When using criteria B1 and B2 with degradation model 3 it was noticed that criteria B2 gave much lower values than criteria B1 for the pure bearing case; this under prediction might be due to the combined effect of the shear term in the fibre tensile criterion of B2 and the degradation model 3, which turned out to be more aggressive than degradation model 2. When comparing criteria B1 with degradation models 2 and 3, the fact that degradation model 3 reduces the stiffness by 90% does have a clear effect. It was observed that by defining different degradation percentages for the different failure mechanisms, it allows the criteria to predict higher failure loads. This observation also agrees with Tserpes [47]. In addition, in degradation model 3, for the matrix tensile and matrix compressive failure mechanism, the shear modulus, G_{12} , and the Poisson's ratio, ν_{12} , are reduced, whereas in degradation model 2 they are not affected. This might also explain why criteria B1 and B2 with degradation model 3 gave slightly lower values in pure bearing than criteria B1 and B2 with degradation model 2.

Group C

Figures 8 and 9 show the results obtained for different bearing versus bypass loading cases for group C. All of them are two-dimensional Hashin type failure criteria. As expected, criteria C1 over-predicted failure in bearing and bypass dominant loads since they were proposed for open plates in compression. They include matrix tensile and compressive failure as well as fibre-matrix shear-out failure mechanisms, but do not consider a fibre tensile

criterion. The lack of this criterion makes criteria C1 unsuitable for bearing versus bypass analysis. Figure 8 shows that criteria C2, C3 and C4 predicted the same failure point for pure bearing and the 20 kN bypass cases. Criteria C2 and C3 are the only ones that include the Hashin fibre tensile failure criterion (equation 19). In this case the damage parameter included in these 3 criteria continuously reduces the value of the shear modulus thus decreasing the shear stresses and allowing the laminate to support higher loads, this behaviour agrees with that observed by Dano et al [44], however in this work failure load predictions for bearing dominant loads agree with experimental results. This might be due to the degradation models being more stable. Criteria C4 do not include the shear term in the fibre tensile criterion thus supporting high tensile load comparable to criteria C2 and C3.

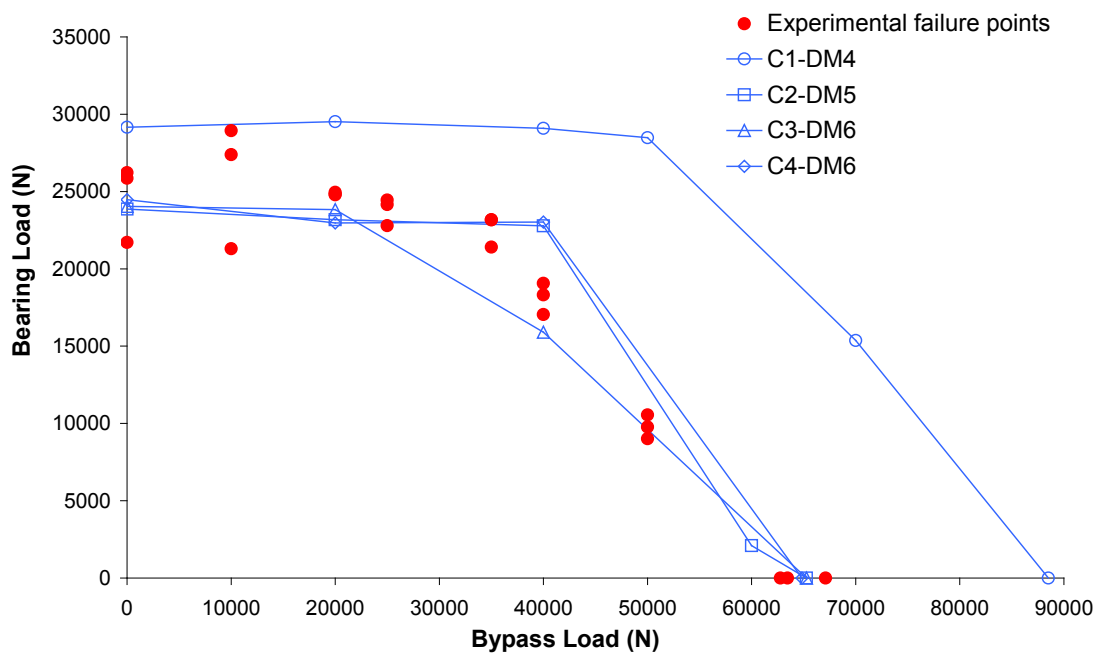


Figure 8 - Bearing versus bypass curves for group C. Two-dimensional Hashin type failure criteria. Degradation models 4, 5 and 6.

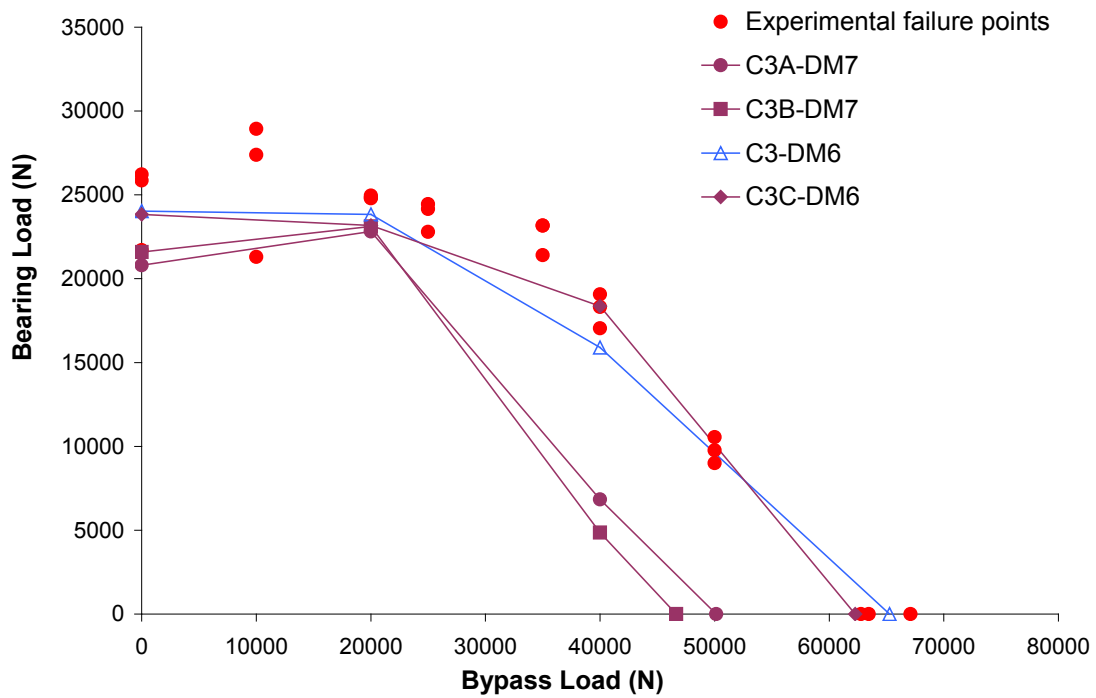


Figure 9 - Bearing versus bypass curves for modified group C3. Two-dimensional Hashin type failure criteria. Degradation models 6 and 7.

It is also observed that criteria C3 is very similar to criteria C2, but criteria C3 do not include the fibre matrix shear failure mechanism. It is clear, from Figure 8, that criteria C3 predict lower (better) values than criteria C2 and C4 at 40 kN bypass. This behaviour might be attributed to the fibre matrix shear failure mechanism. In all degradation models fibre matrix shear is related to the shear modulus, when this mechanism is present in failure criteria that consider the damage parameter the shear modulus is further reduced (reducing the shear stresses for a given tensile load). However if this criterion is not considered (criteria C3) the high shear stresses developed are reduced only by the damage parameter. This theory might also explain why criteria C4 gave higher values than criteria C3. In this case although criteria C4 do not include the fibre matrix shear failure mechanism, the fibre tensile criterion does not consider the high shear stresses developed, thus allowing the laminate to take more load. Since fibre-matrix shear failure is driven by compressive stresses, it is observed in Figure 8 that the effects of the fibre matrix shear in criteria C2, at pure bypass loads, is insignificant or not present thus leaving the behaviour of the shear stresses to the shear non-linearity parameter (d). Nevertheless, a more detailed study of the effect of fibre matrix shear and fibre tensile mechanisms on the failure predictions at high bypass stresses is recommended.

Figure 9, shows the effect of the shear non-linear behaviour term (criteria C3B) and the shear damage parameter (criteria C3C). It is clear that the shear damage parameter improves results, as aforementioned the shear damage parameter reduces the shear stresses by reducing the shear modulus; this action enables the laminate to support more load (C3 and C3C). When the shear damage parameter is not present, the shear non-linear term slightly improved results for the pure bearing case when compared to criteria C3A, but surprisingly, this term tended to reduce the ultimate failure load at high bypass stresses, which contradicts the finding for criteria A2.

Figure 10 shows the failure criteria and degradation models that best predicted failure. It is observed that the reason why two-dimensional criteria predict reasonable results might be due to the inclusion of the shear damage parameter and the lack of out-of-plane shear terms and the delamination failure criterion. Nonetheless, it is important to recognize that bearing failure is a three-dimensional phenomenon [13, 18, 31, 43, 47] which is affected by different parameters such as friction, stacking sequence, clamping forces and delamination and the use of two-dimensional criteria has to be taken with care.

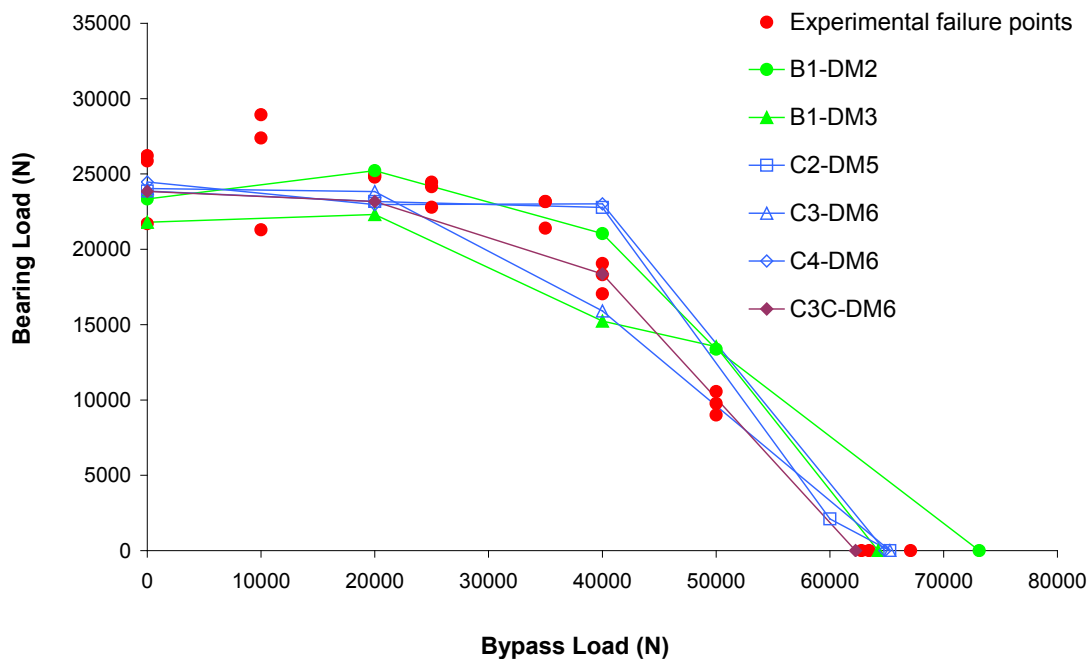



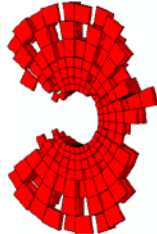

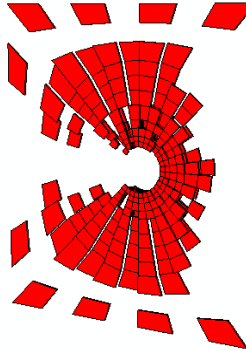











Figure 10 - Bearing versus bypass curves for group B and C. Two and three-dimensional Hashin type failure criteria. Degradation models 2, 3, 5 and 6.

Damage results for models A2-DM2, B1-DM2, B2-DM2 and C3C-DM7

In Tables 13 and 14 the damage generated for the different failure mechanisms is presented for four different models at the point that the extent of fibre tensile failure damage around the hole had reached the failure criterion of 3.5mm with a bypass load of 20kN. When comparing models B1 and B2, utilising degradation model 2, it can




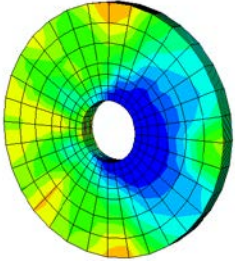
be seen that the extent of damage in model B1 is much greater than in model B2. As discussed earlier this is due to shear terms being added to the fibre failure criterion of model B2, which causes fibre damage to progress more rapidly and prevents other types of damage occurring prior to reaching the 3.5mm fibre failure condition.

Table 13 - Extent of fibre and matrix tensile and compressive failure, at the point that fibre tensile or compressive failure exceeds 3.5mm from the hole edge.

Criteria	A2-DM2	B1-DM2	B2-DM2	C3C-DM6
Bypass Load	20.00 kN	20.00 kN	20.00 kN	20.00 kN
Bearing Load	14.83 kN	25.19 kN	9.04 kN	23.82 kN
Pin Displacement	(0.00065453 m)	(0.0009368 m)	(0.000307009 m)	(0.001197456 m)
Failure Mode	Fibre Tensile Failure @ 0°	Fibre Tensile Failure @ 0°	Fibre Tensile Failure @ 0°	Fibre Tensile Failure @ 0°
Matrix Tensile Failure				
Matrix Compressive Failure				
Fibre Tensile Failure				
Fibre Compressive Failure				

The failure criteria for model A2 are quite different to models B1 and B2 with no de-lamination or fibre shear out failure and different formulations for matrix tensile, matrix compressive and fibre tensile failure. Model B2 though is similar to model A2 in that it contains shear terms in the fibre tensile failure criterion. The results are similar to model B2 which can probably be accounted for by the inclusion of the shear terms in the fibre tensile failure criterion.

Table 14- Extent of fibre matrix shear damage, de-lamination and shear non-linearity damage, at the point that fibre tensile or compressive failure exceeds 3.5mm from the hole edge.

Criteria	A2-DM2	B1-DM2	B2-DM2	C3C-DM6
Bypass Load	20.00 kN	20.00 kN	20.00 kN	20.00 kN
Bearing Load	14.83 kN	25.19 kN	9.04 kN	23.82 kN
Pin Displacement	(0.00065453 m)	(0.0009368 m)	(0.000307009 m)	(0.001197456 m)
Failure Mode	Fibre Tensile Failure @ 0°	Fibre Tensile Failure @ 0°	Fibre Tensile Failure @ 0°	Fibre Tensile Failure @ 0°
Fibre-Matrix Shear	Not considered			Not considered
Delamination	Not considered		NO-DAMAGE	Not considered
Shear Non – Linearity Damage	Not considered	Not considered	Not considered	

Comparing the damage of model C3C with models A2, B1 and B2 in tables 13 and 14 must be done with care as not only are the damage criteria different but also the degradation model used is different. The results for model C3C are similar to model B1. We might have expected model C3C to give similar results to models A2 and B2 as there is a shear term included in the fibre tensile failure criterion, which caused early failure in models A2 and B2. It would appear though that the effect of the shear term in the fibre tensile failure criterion is being mitigated in model C3C by the shear non-linearity damage term which reduces the shear stiffness values. This seems to slow down the fibre tensile failure whilst causing more fibre matrix failure.

CONCLUSIONS

Different stress-based failure criteria and degradation models have been applied to predict the final failure load and damage extension in a pin-jointed laminate subjected to variable bearing versus bypass loads. The criteria factors that had greatest effect were the shear term in Hashin's fibre tensile criterion and the shear non linearity damage parameter. It was observed that the use of the Hashin type fibre tensile criterion may underestimate

failure at bypass dominant loads if the damage parameter (shear-stress shear-strain nonlinearity) is not considered (Figure 7, 9). Moreover, if this damage parameter is considered when including the fibre matrix shear failure mechanism, predictions tend to slightly over-estimate failure (Figure 8). Additionally, it was also noticed that changes in the post-initial failure degradation model had an important effect in the ultimate load prediction and that gradual degradation resulted in a more stable analysis giving improved results. The mesh convergence demonstrated that models with fewer elements gave very similar results to those with higher mesh densities. Furthermore, the criterion proposed to assess the final failure point (radial damaged distance) seems to provide very good results for all the failure criteria tested. The damage extension Figures in Table 12 showed a clear change in failure mode for the different bearing versus bypass cases. It was observed that fibre compressive failure diminishes as the bypass load increases until it completely disappears in the pure bypass case. It is also clear that the tensile failure modes diminish as bearing forces become dominant.

The best overall failure predictions obtained were those made by criteria sets B1, C2, C3 and C4. However it is very important to notice that criteria in group C are two-dimensional and they do not consider delamination, which is an important failure mechanism. Criteria B1 with degradation model 2 was shown to be a very good choice among the different criteria tested, despite the fact that non-linear shear behaviour and the non-linear damage parameter were not considered. It is recommended though, that these parameters be considered in any laminate containing off-axis orientated layers [45]. All of the degradation models apart from model 2 reduce the material properties by 90% of their original value. This would seem a reasonable approach if this value is the lowest that can be reached whilst maintaining stability. Degradation model 2 [30] on the other hand varies the amount of reduction from 60% to 93% depending on the property and the failure criterion. There does not seem to be much basis for why this variation should be used and is questionable without some physical basis for the choices.

ACKNOWLEDGMENTS

The authors would like to thank the support of AIRBUS (UK) Ltd who supplied some of the composite materials used in this work and gave technical advice and CONACyT (National Council for Science and Technology), Mexico, for student financial support.

REFERENCES

1. Hartsmith LJ. Bolted Joints in Graphite/Epoxy Composites. NASA CR144899, 1977.
2. Garbo SP, Ogonowski JM. Effects of Variances and Manufacturing Tolerances on the Design Strength and Life of Mechanically Fastened Joints. Air Force Flight Dynamics Laboratory AFFDL-TR-78-179, 1978.
3. Crews JH, Naik RA. Combined Bearing and Bypass Loading on Graphite/Epoxy Laminate. *Composite Structures*. 1986; 6: 21-40.
4. Oplinger DW. Bolted Joints in Composite Structures – An Overview. 83rd Meeting of AGARD SMP. 1996; 1-11.
5. Chang F-K, Scott RA, Springer GS. Failure of Composite Laminates Containing Pin Loaded Holes. *Journal of Composite Materials*, 1984; 18: 255-278.
6. Prabhakaran R, Razzaq Z, Devara S. Load and Resistance Factor Design (LRFD) Approach for Bolted Joints in Pultruded Composites. *Composites Part B*, 1996; 27B: 351-360.
7. Starikov R, Schon J. Quasi-static Behaviour of Composite Joints with Protruding-head Bolts, *Composite Structures*, 2001; 25: 556-577.
8. Prabhakaran R, Razzaq Z, Devara S. Load and Resistance Factor Design (LRFD) Approach for Bolted Joints in Pultruded Composites. *Composites Part B*, 1996; 27B: 351-360.
9. Blackie AP, Chutima S. Stress Distribution in Multi Fastened Composite Plates, *Composite Structures*, 1996; 34: 427-436.
10. Lin W-H, Jen M-H. The Strength of Bolted and Bonded Single Lapped Composite Joints in Tension. *Journal of Composite Materials*, 1999; 33: 640-666.
11. Xiaopen W, Ling Y. Effect of Joint Parameters, Patterns and Interference on the Bolt Loading in Composite Multi-bolt Joints. *Int. Conf. on Composite Structures*, 1991; 519-530.
12. Ireman T. Three-dimensional stress analysis of bolted single-lap composite joints. *Composite Structures*, 1998; 43: 195-216.
13. Sun H-T, Chang F-K & Qing X. The response of composite joints with bolt-clamping loads, part I: Model development. *Journal of Composite Materials*, 2002; 36: 47-67.
14. Perugini P, Riccio A and Scaramuzzino F. Three-Dimensional Progressive Damage Analysis of Composite Joints. *Proceedings of the 8th International Conference on Civil and Structural Engineering Computing*. Civil-Comp Press, 2001; 18-21.

15. Kermanidis T, Labeas G, Tserpes KI, Pantelakis S. Finite Element Modelling of Damage Accumulation in Bolted Composite Joints under Incremental Tensile Loading. ECCOMAS, 2000; 1-14.
16. Chen H-W, Lee S-S. Numerical and Experimental Failure Analysis of Composite Laminates with Bolted Joints under Bending Loads. *Journal of Composite Materials*, 1995; 29: 15-35.
17. Chen H-W, Lee S-S, Yeh J-T. Three Dimensional Contact Stress Analysis of a Composite Laminate with Bolted Joint. *Journal of Composite Materials*, 1995; 30: 287-297.
18. McCarthy CT, McCarthy MA, Lawlor VP. Progressive damage analysis of multi-bolt composite joints with variable bolt-hole clearances. *Composites: Part B*, 2005; 36: 290-305.
19. Zarco-González JC, Fellows NA, Durodola JF. A step-size independent method for finite element modelling of damage in composites, *Composite Science and Technology*, 2004; 10-11:1679-1689.
20. Zarco-González, JC, Fellows NA, Durodola JF. Design of a composite by-pass versus bearing testing apparatus, *Review of Scientific Instruments*, 2003; 9: 4194-4198.
21. Zarco-González JC. Analysis of damage progression in composites joints subjected to bearing and bypass loads. 2005. PhD Thesis, Oxford Brookes University, Oxford UK.
22. Hinton MJ, Soden PD, Kaddour AS. A comparison of the predictive capabilities of current failure theories for composite laminates. *Composites Science and Technology*, 1998; 58: 1225-1254.
23. Hinton MJ, Soden PD, Kaddour AS. On the maturity of world-wide failure theories: comparison with experiments for +/- 55 GRP laminates. ICCM-Proceedings. 12th International Conference on Composite Materials, 1999. 5-9th July. Paris, France.
24. Hashin Z, Rotem A. A fatigue failure criterion for fibre reinforced materials. *Journal of Composite Materials*, 1973; 7: 448-464.
25. Hashin Z. Failure criteria for unidirectional fiber composites. *Journal of Applied Mechanics*, 1980; 47: 329-334.
26. Rosales-Iriarte F, Fellows NA, Durodola JF. Experimental evaluation of the effect of clamping force and hole clearance on carbon composites subjected to bearing versus bypass loading. *Composite Structures*, 2011; 93: 1096-1102.
27. ABAQUS/Standard Users Manual (2004) Volume II, Version 6.5.
28. F-K Chang, Chang K-Y. A progressive damage model for laminated composites containing stress concentrations. *Journal of composite materials*, 1987; 21, 834-855.

29. Sleight DW. Progressive failure analysis methodology for laminated composite structures. 1999, NASA/TP-1999-209107, Washington DC.
30. Papanikos P, Tserpes KI, Pantelakis S. Modelling of fatigue damage progression and life of CFRP laminates. *Fatigue fracture of engineering materials and structures*, 2003; 26: 37-47.
31. Marshall IH, Arnold WS, Wood J, Mousley RF. Observations on bolted connections in composite structures. *Journal of composite Structures*, 1989; 13: 133-151.
32. Sun H-T, Chang F-K & Qing X. The response of composite joints with bolt-clamping loads, part II: Model verification. *Journal of Composite Materials*, 2002; 36: 69-92.
33. Vangrimde B, Boukhill R. Descriptive relationships between bearing response and macroscopic damage in GRP bolted joints. *Composites: Part B*, 2003; 34: 539-605.
34. Tan SC. A progressive failure model for composite laminates containing openings. *Journal of Composite Materials*, 1991; 25: 556-577.
35. Paris F. A Study of failure criteria of fibrous composite materials. NASA / Langley Research Centre, Hampton, Virginia, 2001; NASA/CR-2001-210661.
36. Tsai SW, Wu EM. A general theory of strength for anisotropic materials. *Journal of Composite Materials*, 1971; 5, 58-80.
37. Yamada SE, Sun CT. Analysis of laminate strength and its distribution. *Journal of Composite Materials*, 1978; 12, 275-284.
38. O'Higgins RM, Padhi GS, McCarthy MA, McCarthy CT. Experimental and numerical study of the open-hole tensile strength of carbon/epoxy composites. *Mechanics of Composites Materials*, 2004; 40: 269-278.
39. Chang F-K, Scott RA, Springer GS. Failure strength of nonlinearly elastic composite laminates containing a pin loaded hole. *Journal of Composite Materials*, 1984; 18: 464-477.
40. Chang F-K, Chang K-Y. Post-Failure analysis of bolted composite joints in tension or shear-out mode failure. *Journal of Composite Materials*, 1987; 21: 809-833.
41. Hashin Z. Fatigue failure criteria for unidirectional fibre composites. *Journal of Applied Mechanics*, 1981; 48: 846-852.
42. Ye L. Role of matrix resin in delamination onset and growth in composite laminates. *Composites Science and Technology*, 1988; 33: 257-277.

43. Tserpes KI, Papanikos P, Kermanidis T. A three-dimensional progressive damage model for bolted joints in composite laminates subjected to tensile loading. *Fatigue and Fracture of Engineering Materials and Structures*, 2001; 24: 663-675.
44. Dano M-L, Gendron G, Picard A. Stress and failure analysis of mechanically fastened joints in composite laminates. *Composite Structures*, 2000; 50: 287-296.
45. Hahn HT, Tsai SW. Nonlinear elastic behaviour of unidirectional lamina. *Journal of Composite Materials*, 1973; 7: 102-118.
46. Chang F-K, Lessard LB. Damage tolerance of laminated composites containing an open hole and subjected to compressive loadings: Part I – Analysis. *Journal of Composite Materials*, 1991; 25: 2-43.
47. Tserpes KI, Papanikos P, Kermanidis T. Strength prediction of bolted joints in graphite/epoxy composite laminates. *Composites: Part B*, 2002; 33: 521-529.
48. Choi J-H, Chun Y-J. Failure Load Prediction of Mechanically Fastened Composite Joints. *Journal of Composite Materials*, 2003; 37: 2163-2177.
49. Hung CL, Chang F-K. Bearing failure of bolted composite joints. Part II: Model and verification. *Journal of Composite Materials*, 1996; 30: 1359-1400.
50. Camanho PP, Matthews FL. A progressive damage model for mechanically fastened joints in composite laminates. *Journal of Composite Materials*, 1999; 33: 2248-2280.
51. Quinn WJ, Matthews FL. The effect of stacking sequence on the pin-bearing strength in glass fibre reinforced plastic. *Journal of Composite Materials*, 1977; 11: 139-145.
52. Ireman T, Ranvik T, Eriksson I. On damage development in mechanically fastened composite laminates. *Composite Structures*, 2000; 49: 151-171.
53. Herrington PD, Sabbaghian M. Effect of radial clearance between bolt and washer on the bearing strength of composite bolted joints. *Journal of Composite Materials*, 1993; 26: 1826-1843.
54. Ascione F, Feo L, Maceri F. An Experimental Investigation on the Bearing Failure Load of Glass/epoxy Laminates. *Composites: Part B*. 2009; 40: 197-205
55. Ascione F, Feo L, Maceri F. On the Pin-bearing Failure Load of GFRP Bolted Laminates: An experimental analysis on the influence of bolt diameter. *Composites: Part B*. 2010; 41: 482-490